










## Open Archive Toulouse Archive Ouverte (OATAO)

OATAO is an open access repository that collects the work of Toulouse researchers and makes it freely available over the web where possible

This is a Publisher's version published in: <http://oatao.univ-toulouse.fr/23571>

**Official URL:** <https://doi.org/10.5281/zenodo.1187512>

### To cite this version:

Hernández-López, Ana Maria  and Guillemet, Sophie  and Valdez Nava, Zarel   
and Aguilar-Garib, Juan Antonio and Tenailleau, Christophe  and Dufour,  
Pascal  and Demai, Jean-Jacques  and Durand, Bernard  *Influence of Y2O3 on  
the structure of Y2O3-doped BaTiO3 powder and ceramics.* (2018) International  
Journal of Engineering Research & Science, 4 (2). 7-11. ISSN 2395 - 6992

Any correspondence concerning this service should be sent  
to the repository administrator: [tech-oatao@listes-diff.inp-toulouse.fr](mailto:tech-oatao@listes-diff.inp-toulouse.fr)

# Influence of $Y_2O_3$ on the structure of $Y_2O_3$ -doped $BaTiO_3$ powder and ceramics

Ana María Hernández-López<sup>1</sup>, Sophie Guillemet-Fritsch<sup>2</sup>, Zarel Valdez-Nava<sup>3</sup>, Juan Antonio Aguilar-Garib<sup>4</sup>, Christophe Tenailleau<sup>5</sup>, Pascal Dufour<sup>6</sup>, Jean-Jacques Demai<sup>7</sup>, Bernard Durand<sup>8</sup>

<sup>1</sup>CICFIM, Universidad Autónoma de Nuevo León, San Nicolás de los Garza, N.L., MX 66455.

<sup>1,2,5,6,7,8</sup>CIRIMAT, Université de Toulouse, CNRS, Université de Toulouse 3-Paul Sabatier, 118 route de Narbonne, 31062, Toulouse Cedex 9, France.

<sup>3</sup>LAPLACE, Université de Toulouse, CNRS, INPT, UPS, France.

<sup>4</sup>Universidad Autónoma de Nuevo León, FIME, San Nicolás de los Garza, N.L., MX 66455.

**Abstract**—Barium titanate ( $BaTiO_3$ ) doped with rare-earth elements (REE) is used as dielectric in the manufacture of multilayer ceramic capacitors (MLCCs). The most common REE oxide employed as dopant for this application is  $Y_2O_3$ . The behavior of the  $Y^{3+}$  in the  $BaTiO_3$  structure depends on its concentration and the sintering conditions, among other factors, which can induce the formation of secondary phases that are a potential cause a detriment to the electrical properties of  $BaTiO_3$ . The purpose of this work is to perform a phase characterization of  $BaTiO_3$  doped with different concentrations of  $Y_2O_3$ , validating its possible contribution to the formation of secondary phases. The role of  $Y_2O_3$  was evaluated on two kinds of raw materials. The first one is pure  $BaTiO_3$  (< 100 ppm Y) and the second kind is a commercial formulation designed for MLCCs known as X7R (-55°C and 125°C, 15% tolerance), which among other elements, already contained 1 wt% of  $Y_2O_3$ . High concentrations of  $Y_2O_3$  (1% up to 20 wt%) were used aiming to promote structural changes, and even the formation of secondary phases in amounts suitable to be detected by X-ray diffraction. Heat treatment of powder and sintering of ceramics (powder compacted at 2 MPa) were conducted in air (1310°C in air for 3 h, two steps: 1350°C then 1150°C 15 h). A phase transition from tetragonal to a mixture of tetragonal and cubic was observed as  $Y_2O_3$  concentration increases in the thermally treated powder and in the corresponding ceramics. Commercially formulated powder showed higher densification than pure  $BaTiO_3$ , and produced cubic structure at higher  $Y_2O_3$  concentrations. The phase  $Ba_6Ti_{17}O_{40}$  is detected in the 20 wt%  $Y_2O_3$ -doped sample.

**Keywords**— $BaTiO_3$ , doping,  $Y_2O_3$ .

## I. INTRODUCTION

$BaTiO_3$  presents interesting electromagnetic properties and has become the main component of the formulation of the dielectric material for multilayer ceramic capacitors (MLCCs) [1, 2]. The formulation used in this application must be designed to control the electromagnetic properties of the layer, especially at high temperature and under high electric field [3,4]. For this purpose, several additives and dopants are added to  $BaTiO_3$ . They include cations such as Mn, Mg and Ca, that can partially compensate the electrons and holes that the system might contain, due to the presence of oxygen vacancies [3, 5]. They also include sintering aids, such as  $SiO_2$ , which reduce the sintering temperature. Indeed, it has been reported that  $SiO_2$  leads to formation of a liquid phase from the ternary system  $BaO$ - $TiO_2$ - $SiO_2$ , diminishing the eutectic point from 1320°C to near 1260 °C [6,7]. Finally, REE are added,  $Dy^{3+}$ ,  $Ho^{3+}$ ,  $Sm^{3+}$ ,  $La^{3+}$ ,  $Yb^{3+}$  or  $Y^{3+}$ . They substitute Ba and Ti cations in the  $BaTiO_3$  structure [8, 9]. However, in particular,  $Dy^{3+}$ ,  $Ho^{3+}$  and  $Y^{3+}$ , have shown an amphoteric behavior (occupying A- or B-site) and they are described as helpful for the lifetime of the MLCCs [1].  $Y_2O_3$  is commonly employed as dopant in the commercial formulation of powder for fabrication of MLCCs, because at industrial scale. It results in similar properties than adding  $Ho_2O_3$ ,  $Er_2O_3$  or  $Dy_2O_3$ , and it is less expensive [8]. Dopants also take part in the formation a so-called “core-shell” structure that is claimed to contribute to the temperature stability of the dielectric properties [8-11].  $Y_2O_3$  ionic radius (0.107 nm) is intermediate between that of the  $Ba^{2+}$  ion (0.161 nm) and the  $Ti^{4+}$  ion (0.06 nm). Therefore  $Y^{3+}$  can take either  $Ba^{2+}$  or  $Ti^{4+}$  cation site in the  $BaTiO_3$  lattice [1, 2], and can behave as acceptor or donor according to the position in the lattice. The energy required to form a  $Ti^{4+}$  vacancy in the  $BaTiO_3$  lattice is 7.56 eV whereas it is only 5.94 eV to form a  $Ba^{2+}$  vacancy [12-14]. The partial pressure of oxygen and sintering temperature will also induce the formation of  $Ba^{2+}$  or  $Ti^{4+}$  vacancies, leading  $Y^{3+}$  to occupy either one or both of them [12, 14]. This will be influenced also by the Ba/Ti ratio, the dopant concentration and its solubility, which varies according to  $Y^{3+}$  taking either the Ba- or the Ti-site. Zhi et al. [15] indicated a solubility of  $Y^{3+}$  at the Ba-site of about 1.5 at% when sintering in air at 1440 – 1470°C, while it reaches 4 at%

when sintering under reducing conditions [16]. For the Ti-sites instead, the solubility is higher  $\approx 12.2$  at% at  $1515^\circ\text{C}$  when sintering in air. Wang et al. [2] reported that the introduction of  $\text{Y}^{3+}$  in the  $\text{BaTiO}_3$  lattice, can lead to structural changes, as phase transformation from tetragonal to cubic. Also, it has been observed that the solid solubility of the dopant in the  $\text{BaTiO}_3$  is surpassed, when secondary phases are formed as precipitates. In the case of  $\text{Y}^{3+}$ , Belous et al. [17] reported the formation of the  $\text{Ba}_6\text{Ti}_{17}\text{O}_{40}$  and  $\text{Y}_2\text{Ti}_2\text{O}_7$  as secondary phases. The pyrochlore phase  $\text{Y}_2\text{Ti}_2\text{O}_7$  was evidenced by Yoon et al. [3] and Zhang et al. [8] and they suspected that these phases are detrimental to the reliability of  $\text{BaTiO}_3$ -based MLCCs.

In most industrial processes the dopant level is below 1 wt% [12] and the sintering is performed in a reducing atmosphere. Whereas in this research, doping levels are much higher and sintering is carried out in air. To understand the role of  $\text{Y}^{3+}$  addition in the formation of second phases a large range of dopants levels need to be explored up to and above the solubility limit. In this work we aim to investigate the structural changes of  $\text{BaTiO}_3$  structure when adding  $\text{Y}_2\text{O}_3$ , induced by high doping levels ( $>1$  wt%) when sintering is performed under air.

## II. MATERIALS AND METHODS

Powder of  $\text{BaTiO}_3$  doped with  $\text{Y}_2\text{O}_3$  was prepared (according to the formula  $\text{Ba}_{1-x}\text{Y}_x\text{Ti}_{1-x/4}\text{O}_3$ ) by traditional solid state reaction. Two types of  $\text{BaTiO}_3$  were used, “BT-A” with commercial reagent-grade purity (Ferro Electronic Materials Inc.), and “BT-B” with formulated composition for its application in MLCCs production, containing additives, mainly:  $\text{Y}_2\text{O}_3$ : 1.05%;  $\text{SiO}_2$ : 0.30%,  $\text{CaO}$ : 1.34%). Each  $\text{BaTiO}_3$  powder was mixed with the necessary amount of  $\text{Y}_2\text{O}_3$  to obtain doped samples at 2.5, 5 and 20 wt%, then they were ball-milled in a polyurethane mill bottle with yttrium-stabilized zirconia balls, using ethanol as the grinding media for 4h.

With the aim to observe any structural change induced by doping, the powder ( $x = 2.5$  to 20 wt%) was thermally treated at  $1310^\circ\text{C}$  in air atmosphere for 3h. Ceramics were prepared with the powder containing 2.5 and 5 wt%  $\text{Y}_2\text{O}_3$ . Then the powder was dried, 1 wt% polyvinyl butyral (PVB) was added to the powder that were mixed, grinded and sieved. Finally it was compacted using uniaxial pressing, producing discs of 8 mm in diameter. The green discs were sintered in air using a tube furnace, under a two-step sintering protocol which reached  $1350^\circ\text{C}$  and then remained at  $1150^\circ\text{C}$  for 15 h.

The crystalline phase of powder and sintered samples was characterized by X-ray diffraction (XRD, Model D4 Endeavor, Bruker AXS), using the  $\text{Cu-}\alpha$  ( $\lambda = 1.54 \text{ \AA}$ ) radiation in the  $2\theta$  range  $10 - 80^\circ$ . The bulk density of the ceramics was determined from the samples mass and geometry. Powder morphology was analyzed by scanning electron microscopy (SEM, JSM-6510LV, JEOL). The particles size was determined from the micrographs using Image J software.

## III. RESULTS AND DISCUSSION

The crystal structure and the densification of the different samples are shown in Table 1.

TABLE 1  
IDENTIFICATION, CHEMICAL COMPOSITION AND STRUCTURE OF THE STUDIED SAMPLES

BaTiO <sub>3</sub> raw material	Y <sub>2</sub> O <sub>3</sub> wt%	Sample ID	Crystalline structure <sup>a</sup>		Secondary phase	Densification (%)
			Powder	Ceramic		
BT-A (reagent-grade)	0	A0	T	T	--	93.7
	2.5	A2.5	T	T+C	--	60.8
	5	A5	T	T+C	--	61.0
	20	A20	T+C	--	--	--
BT-B (commercially formulated)	1	B1	T	T+C	--	96.2
	2.5	B2.5	T+C	C	--	80.1
	5	B5	T+C	C	--	72.6
	20	B20	T+C	--	Ba <sub>6</sub> Ti <sub>17</sub> O <sub>40</sub>	--

<sup>a</sup>Preponderant phase. T: Tetragonal; C: Cubic.

### 3.1 BaTiO<sub>3</sub> Powder

SEM images of the undoped  $\text{BaTiO}_3$  powder, A0 and B1, (Fig. 1 (a and c, respectively)) show that both powder present particles with a coarse-faceted morphology. Two sizes of particles are observed, a range of particles average size of  $0.48 \mu\text{m}$  and  $1.25 \mu\text{m}$  for the A0 and of  $0.46 \mu\text{m}$  and  $0.81 \mu\text{m}$  for the B1. Although the values are close the maximum average value of the B1 particles is lower than the one of the A0 particles, which is due to the thermal treatment given to the formulated powder, as requirement for its use in the MLCCs production process. On the other hand, the SEM pictures of the 5 wt%

$\text{Y}_2\text{O}_3$ -doped  $\text{BaTiO}_3$  powder thermally treated (Fig. 1 (b and d)), show more spherical and defined particles, compared to the undoped powder. They present a more uniform size (A5:  $0.58\ \mu\text{m}$  and B5:  $0.53\ \mu\text{m}$ ) and it is possible to observe aggregates, which might evidence an incipient sintering during the applied thermal process at  $1310^\circ\text{C}$ .

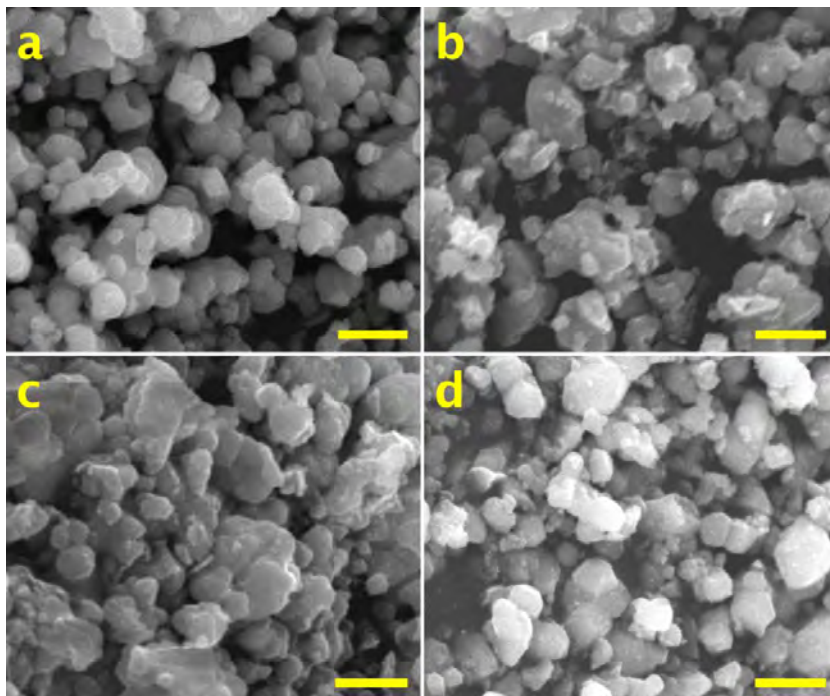


**FIG. 1.** SEM images of undoped  $\text{BaTiO}_3$ : (a) A0, (c) B1 and 5 wt%  $\text{Y}_2\text{O}_3$  (TT): (b) A5, (d) B5 powder. (TT: Thermally treated). Scale bar:  $1\ \mu\text{m}$ .

X-ray diffraction patterns corresponding to the thermally treated powder are presented in Fig.2. Diffraction patterns of powder obtained from the BT-A [(a) A0, A2.5, A5 and A20] fit well with the tetragonal phase. The insets in Fig. 2.a show the peaks associated to the (111) as well as (002)(200) planes of this phase. Further, on the inset of the diffraction peak at  $2\theta$  about  $45^\circ$ , the split in two peaks, is characteristic of a tetragonal phase [2]. For the A20 powder, the planes (002) and (200) suffer a slight distortion and the plane (111) shifts to a lower angle. Moreover for the A5 and A20 samples, the peaks corresponding to  $\text{Y}_2\text{O}_3$  appear, meaning that at least a part of it remains free outside of the  $\text{BaTiO}_3$  lattice, indicating that the solubility limit was surpassed. The shift to lower angles of some peaks is related to an expansion of the unit cell volume due to the substitution of  $\text{Ba}^{2+}$  by  $\text{Y}^{3+}$  ions.

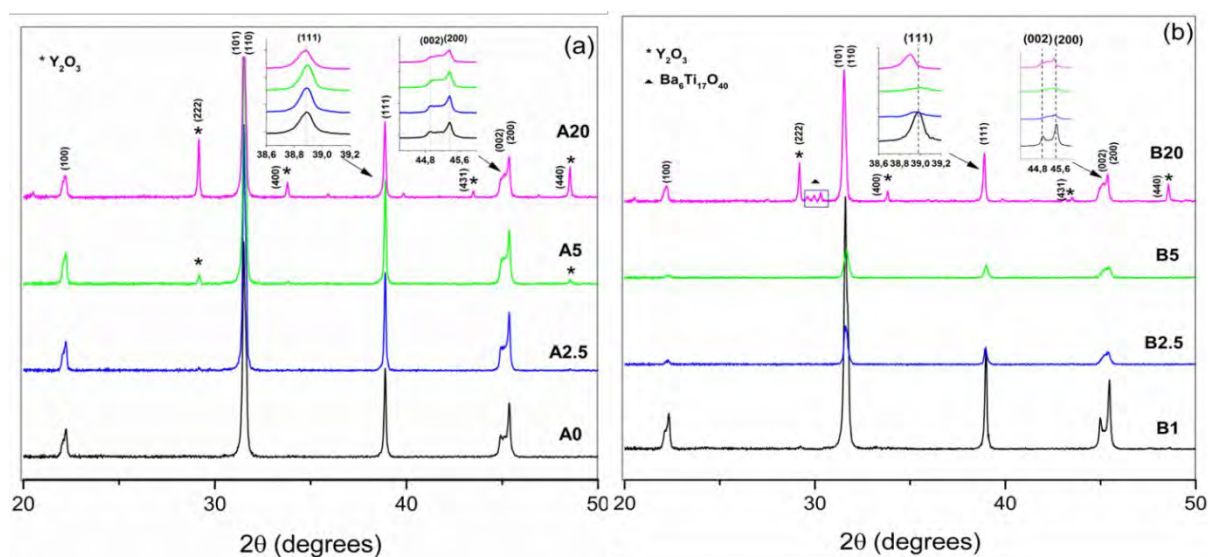


**FIG. 2.** X-ray diffraction patterns of undoped  $\text{BaTiO}_3$  ( $1350^\circ\text{C}$ ) and  $\text{Y}_2\text{O}_3$  - 2.5, 5 and 20 wt% - doped  $\text{BaTiO}_3$  ( $1350^\circ\text{C}$ ) powder. Powder coming from (a) BT-A and (b) BT-B.

On the other hand, the XRD patterns corresponding to the BT-B powder show more changes according to the increasing  $Y_2O_3$  concentration. In this case, the raw material already contains about 1 wt% of  $Y_2O_3$ . The pattern of powder B1 clearly shows a tetragonal phase, whereas those of powder B2.5, B5, and B20 evidence a mixture of tetragonal and cubic phases. For the B20 powder the split of (002) and (220) is more clear than for powder B2.5 and B5 and a shift to lower angle of the (111) peak is also noticed. Contrary to the A samples, the peaks corresponding to  $Y_2O_3$  are detected only for the powder B20, implying the remaining of most of it as a free oxide. Moreover, for B20, three additional peaks appear between  $2\theta \approx 29.5 - 30^\circ$ . They do not match with the  $BaTiO_3$  nor with the  $Y_2O_3$  phases. They could be attributed to the interaction of the  $Y_2O_3$  excess with the  $BaTiO_3$  matrix in conjunction with that of the additives already present. Considering the possible formation of secondary phases when the solubility of  $Y_2O_3$  has exceeded the limit of 1.5 at% for the Ba-site and 12.3 at% for the Ti-site (in air atmosphere) [15], a screening for secondary phases was made, finding a match with  $Ba_6Ti_{17}O_{40}$  (JCPDS 35-0817).  $BaTiO_3$  and  $TiO_2$  are likely to form a eutectic around  $1320^\circ - 1330^\circ C$  and if  $SiO_2$  is present, the eutectic point temperature decreases down to  $1245^\circ - 1260^\circ C$  [18, 19]. Even without the presence of a liquid phase [20], the interaction between the dopants and the additives under our experimental conditions, could lead to a Ti-rich phase forming the secondary phase  $Ba_6Ti_{17}O_{40}$ . This second phase has been reported previously [14, 17].

### 3.2 BaTiO<sub>3</sub> Ceramics

Ceramics are prepared by sintering undoped and doped powder, BT-A (A0, A2.5, A5) and BT-B (B1, B2.5, B5), in the conditions described in the previous section.

Fig. 3 shows the X-ray diffraction patterns of the ceramics. The undoped ceramic (A0) crystallizes in a tetragonal phase, while the doped ones (A2.5 and A5) consist in a mixture of cubic and tetragonal perovskite phases as shown in the inset (Fig. 3(a)), zone around  $2\theta \approx 45^\circ$  where the split of the (200) peaks is deformed. The influence of the  $Y_2O_3$  over the  $BaTiO_3$  structure is greater in the case of the ceramics. Comparing the XRD pattern from the B1 powder (Fig. 2 (b)) and the corresponding ceramic (Fig. 3 (b)), it is possible to see (inset  $2\theta \approx 45^\circ$ ) that there is no peak splitting indicating a phase transformation from tetragonal to a cubic [10-12]. The same behavior is observed for B2.5 and B5 ceramics. This behavior points out the strong interaction between additives and dopants added to the  $BaTiO_3$ , which was also observed in the SEM images (Fig. 1 (d)). The way in which the addition of  $Y_2O_3$  affects the  $BaTiO_3$  structure, is also reflected in the densification of the ceramics (Table 1). Even when in both cases (BT-A and BT-B) the densification decreases as the  $Y_2O_3$  concentration increases, the ceramics issued from the BT-B powder present higher densification values. This is not surprising as one of the purposes of the added compounds to the  $BaTiO_3$  powder is to improve its densification.

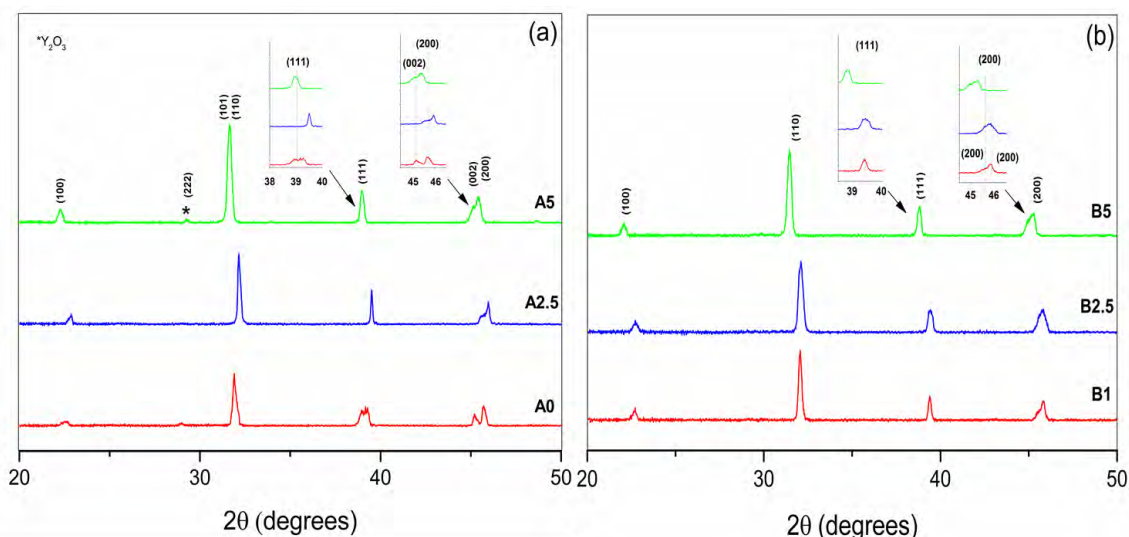


**FIG. 3. X-ray diffraction patterns of undoped BaTiO<sub>3</sub> and Y<sub>2</sub>O<sub>3</sub> - 2.5, 5.0 and 20 wt% - doped BaTiO<sub>3</sub> ceramics. Ceramics resulting from (a) BT-A and (b) BT-B.**

### IV. CONCLUSION

Pure and commercially formulated  $BaTiO_3$  powder was doped with  $Y_2O_3$  by traditional solid state reaction. The  $Y_2O_3$  was added to pure  $BaTiO_3$  and a commercial formulation that already contained 1 wt% of  $Y_2O_3$ , so that final concentrations were 2.5, 5 and 20 wt%. The samples, as powder and as ceramics, were analyzed by XRD. It was observed that as the  $Y_2O_3$



concentration increases, the effects over the BaTiO<sub>3</sub> structure are more evident. The phase transition from tetragonal to a mixture of tetragonal and cubic was observed either in powder thermally treated as in the corresponding ceramics obtained from them. The results indicate that the additives in the commercial formulation have a strong interaction allowing a better densification and a change of phase more than in the powder and ceramics from pure BaTiO<sub>3</sub>. It was even observed the formation of a secondary phase identified as Ba<sub>6</sub>Ti<sub>17</sub>O<sub>40</sub> in the Y<sub>2</sub>O<sub>3</sub>-doped (20 wt%) commercially formulated BaTiO<sub>3</sub> thermally treated powder. No secondary phases formed by BaTiO<sub>3</sub> and Y<sub>2</sub>O<sub>3</sub> were found, free Y<sub>2</sub>O<sub>3</sub> is evidence of surpassing its solubility limit. The changes in the lattice show that Y entered into the lattice, and induces the formation of a secondary phase without Y or other elements of the formulation. These tests were conducted in air, so the oxides were not reduced during the treatments.

### ACKNOWLEDGEMENTS

The authors thank the financial support of the National Science and Technology Council of Mexico (CONACyT) and the Postgraduate Cooperation Program (PCP-RU2I), project 229286, between Mexico and France. We are also grateful with Kemet de México and Marion Technologies, France.

### REFERENCES

- [1] Y. Tsur, T. D., Dunbar, and C. A. Randall "Crystal and defect chemistry of rare earth cations in BaTiO<sub>3</sub>," *J. Electroceram.*, vol. 7, no. 1, pp. 25-34, 2001.
- [2] M. J. Wang, H. Yang, Q. L. Zhang, L. Hu, D. Yu, Z. S. Lin, and Z. S. Zhang "Doping behaviors of yttrium, zinc and gallium in BaTiO<sub>3</sub> ceramics for AC capacitor application," *J. Mater. Sci. Mater. Electron.*, vol. 25, no. 7, pp. 2905-2912, 2014.
- [3] S. H. Yoon, Y. S. J. O. Park, Hong and D. S. Sinn "Effect of the pyrochlore (Y<sub>2</sub>Ti<sub>2</sub>O<sub>7</sub>) phase on the resistance degradation in yttrium-doped BaTiO<sub>3</sub> ceramic capacitors," *J. Mater. Res.*, vol. 22, no. 9, pp. 2539-2543, 2007.
- [4] T. Ashburn, and D. Skamser "Highly accelerated testing of capacitors for medical applications," in Proceedings of the 5th SMTA Medical Electronics Symposium. California, USA, 2008, January.
- [5] S. H. Yoon, S. H. Kang, S. H. Kwon, and K. H. Hur, "Resistance degradation behavior of Ca-doped BaTiO<sub>3</sub>," *J. Mater. Res.*, vol. 25, no. 11, pp. 2135-2142, 2010.
- [6] G. Liu, and R. D. Roseman "Effect of BaO and SiO<sub>2</sub> addition on PTCR BaTiO<sub>3</sub> ceramics," *J. Mater. Sci.*, vol. 34, no. 18, pp. 4439-4445, 1999.
- [7] K. E. Ösküz, M. Torman, S. Sen and U. Sen "Effect of sintering temperature on dielectric properties of SiO<sub>2</sub> Doped BaTiO<sub>3</sub> ceramics," *J. Int. Sci. Publ.: Mater. Methods Technol.*, vol. 10, pp. 361-366, 2016.
- [8] J. Zhang, Y. Hou, M. Zheng, W. Jia, M. Zhu, and H. Yan "The occupation behavior of Y<sub>2</sub>O<sub>3</sub> and its effect on the microstructure and electric properties in X7R dielectrics," *J. Am. Ceram. Soc.*, vol. 99, no. 4, pp. 1375-1382, 2016.
- [9] M. J. Wang, H. Yang, Q. L. Zhang, Z. S. Lin, Z. S., Zhang, D. Yu, D. and L. Hu "Microstructure and dielectric properties of BaTiO<sub>3</sub> ceramic doped with yttrium, magnesium, gallium and silicon for AC capacitor application," *Mater. Res. Bull.*, vol. 60, pp. 485-491, 2014.
- [10] C. H. Kim, K. J. Park, Y. J. Yoon, M. H. Hong, J. O. Hong and K. H. Hur "Role of yttrium and magnesium in the formation of core-shell structure of BaTiO<sub>3</sub> grains in MLCC," *J. Eur. Ceram. Soc.*, vol. 28, no. 6, pp. 1213-1219, 2008.
- [11] K. J. Park, C. H. Kim, Y. J. Yoon, S. M. Song, Y. T. Kim, and K. H. Hur "Doping behaviors of dysprosium, yttrium and holmium in BaTiO<sub>3</sub> ceramics," *J. Eur. Ceram. Soc.*, vol. 29, no. 9, pp. 1735-1741, 2009.
- [12] A. Belous, O. V'yunov, L. Kovalenko, and D. Makovec "Redox processes in highly yttrium-doped barium titanate," *J. Solid State Chem.*, vol. 178, no. 5, pp. 1367-1375, 2005.
- [13] D. Makovec, Z. Samardžija, and M. Drofenik "Solid solubility of holmium, yttrium, and dysprosium in BaTiO<sub>3</sub>," *J. Am. Ceram. Soc.*, vol. 87, no. 7, pp. 1324-1329, 2004.
- [14] M. Paredes-Olguín, I. A. Lira-Hernández, C. Gómez-Yañez and F. P. Espino-Cortes "Compensation mechanisms at high temperature in Y-doped BaTiO<sub>3</sub>," *Physica B*, vol. 410, pp. 157-161, 2013.
- [15] J. Zhi, A. Chen, Y. Zhi, P. M. Vilarinho and J. L. Baptista "Incorporation of yttrium in barium titanate ceramics," *J. Am. Ceram. Soc.*, vol. 82, no. 5, pp. 1345-1348, 1999.
- [16] O. I. V'yunov, L. Kovalenko, A. G. Belous and V. N. Belyakov "Oxidation of reduced Y-doped semiconducting barium titanate ceramics," *Inorg. Mater.*, vol. 41, no. 1, pp. 87-93, 2005.
- [17] A. Belous, O. V'yunov, M. Glinchuk, V. Laguta, and D. Makovec "Redox processes at grain boundaries in barium titanate-based polycrystalline ferroelectrics semiconductors," *J. Mater. Sci.*, vol. 43, no. 9, pp. 3320-3326, 2008.
- [18] S. Senz, A. Graff, W. Blum, D. Hesse and H. P. Abicht "Orientation Relationships of Reactively Grown Ba<sub>6</sub>Ti<sub>17</sub>O<sub>40</sub> and Ba<sub>2</sub>TiSi<sub>2</sub>O<sub>8</sub> on BaTiO<sub>3</sub> (001) Determined by X-ray Diffractometry," *J. Am. Ceram. Soc.*, vol. 81, no. 5, pp. 1317-1321, 1998.
- [19] G. Koschek, and E. Kubalek "On the Electronic Structure and the Local Distribution of the Second Phase Ba<sub>6</sub>Ti<sub>17</sub>O<sub>40</sub> in BaTiO<sub>3</sub> Ceramics," *Phys. Status Solidi A*, vol. 102, no. 1, pp. 417-424, 1987.
- [20] S. J. Zheng, K. Du, X. H. Sang and X. L. Ma "TEM and STEM investigation of grain boundaries and second phases in barium titanate," *Philos. Mag. A*, vol. 87, no. 34, pp. 5447-5459, 2007.